Journal of Solid State Chemistry 182 (2009) 580–585

Contents lists available at ScienceDirect

Journal of Solid State Chemistry

journal homepage: www.elsevier.com/locate/jssc

Synthesis of $Li_{(x)}Na_{(2-x)}Mn_2S_3$ and $LiNaMnS_2$ through redox-induced ion exchange reactions

Joshua A. Luthy, Phillip L. Goodman, Benjamin R. Martin *

Department of Chemistry and Biochemistry, Texas State University—San Marcos, 601 University Drive, San Marcos, TX 78666, USA

ARTICLE INFO

Article history:
Received 20 July 2008
Received in revised form
10 November 2008
Accepted 17 November 2008
Available online 3 December 2008

Keywords:
Reductive intercalation
Oxidative deintercalation
Layered materials
Ion exchange

ABSTRACT

$Na_2Mn_2S_3$ was oxidatively deintercalated using iodine in acetonitrile to yield $Na_{1.3}Mn_2S_3$, with lattice constants nearly identical to that of the reactant. Lithium was then reductively intercalated into the oxidized product to yield $Li_{0.7}Na_{1.3}Mn_2S_3$. When heated, this metastable compound decomposed to form a new crystalline compound, $LiNaMnS_2$, along with MnS and residual $Na_2Mn_2S_3$. Single crystal X-ray diffraction structural analysis of $LiNaMnS_2$ revealed that this compound crystallizes in $P\text{-}3m1$ with cell parameters $a = 4.0479(6)$ Å, $c = 6.7759(14)$ Å, $V = 96.15(3)$ Å^3 ($Z = 1$, w$R2 = 0.0367$) in the $NaLiCdS_2$ structure-type.

1. Introduction

Intercalation reactions of alkali metals into host structures have drawn significant interest mainly due to the potential use of resulting compounds for energy storage devices [1–3]. Such reactions can be performed using a number of techniques, including the direct reaction of an alkali metal with a structure either in the vapor phase or in liquid ammonia [4,5], by reacting a structure with an organoalkali metal reactant such as butyl lithium [6], or through electrochemical reduction in the presence of alkali metal salts [7]. These reductive intercalation reactions may be reversed by oxidatively deintercalating ions from a structure, either through the use of an oxidizing agents like O_2, H_2O_2, or I_2 [8], or by electrochemical cycling [9]. In one of the most dramatic examples of oxidative deintercalation on a chalcogenide, by oxidizing the layered compounds $A_2Bi_4Se_7$ (A = Rb, Cs) with iodine, the alkali metal ions were ejected and the layers were completely knitted together through dichalogenide bonds [10]. Due to the low temperature conditions of these reactions, they may be used to synthesize thermodynamically unstable (but kinetically stable) phases. By combining oxidative deintercalation and reductive intercalation, ions may be cycled in and out of a structure to yield new materials. This allows considerably more control over the resulting product as compared to simple ion exchange reactions, such as the reaction of alkali metal salts with a reactant phase [11], since ions may be mobilized at much lower temperatures.

$Na_2Mn_2S_3$ is a layered structure that crystallizes in space group $C2/c$, with planes of edge- and corner-shared MnS_4 tetrahedra separated by sodium cations (Fig. 1) [12]. The only known isostructural phase is $Na_2Mn_2Se_3$ [13]. This structure type contains two different alkali metal coordination environments: 4-coordiante pseudo-tetrahedral sites located within puckered regions of the $Mn_2S_3^{-2}$ layers (site Na(1) in Fig. 1), and 6-coordinate pseudo-octahedral sites located directly between the $Mn_2S_3^{-2}$ layers (sites Na(2) and Na(3) in Fig. 1).

The oxidative deintercalation of sodium ions from $Na_2Mn_2S_3$ was explored by Koizumi and coworkers through the reaction of the host with iodine in acetonitrile [4]. Based on titration experiments, the following reaction was proposed:

$$Na_2Mn_2S_3 + 1/2\ I_2 \rightarrow NaMn_2S_3 + NaI$$

Although half of the sodium ions were reported to deintercalate from the structure, yielding an average manganese oxidation state of +2.5, the unit cell was not observed to change significantly as a result of this reaction. Since the native structure contains two types of sodium environments, the authors proposed that one of these sites (hypothesized to be the octahedral site) is selectively removed through the oxidation reaction [14]. Although this was justified on the basis of intensity changes in powder XRD data, these data were not presented in the published work.

We discuss here a further exploration of the redox activity of $Na_2Mn_2S_3$, and the use of redox cycling to exchange ions within a chalcogenide structure. The strategy pursued here is to use oxidative deintercalation to initially generate site vacancies in a

* Corresponding author. Fax: +1 512 245 2374.
E-mail address: bmartin@txstate.edu (B.R. Martin).

0022-4596/$ - see front matter © 2008 Elsevier Inc. All rights reserved.
doi:10.1016/j.jssc.2008.11.025

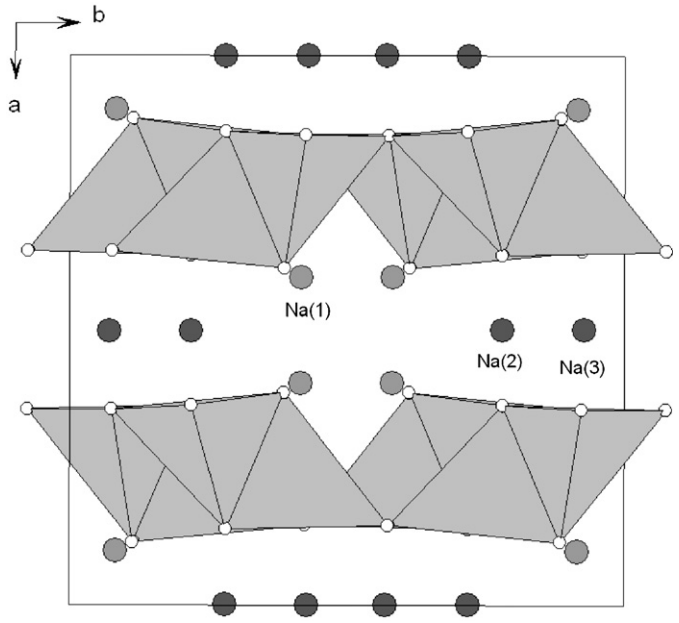

Fig. 1. Structure of $Na_2Mn_2S_3$ viewed along the *c*-axis. Manganese is drawn at the center of gray polyhedra, sulfur is depicted as white spheres, and sodium is shaded in gray (4-coordiante Na(1) sites) or black (6-coordinate Na(2) and Na(3) sites) to distinguish between the different coordination environments.

structure (through the removal of sodium ions). In a subsequent reductive intercalation reaction these vacancies may be filled by a different intercalant (through the incorporation of lithium ions). We examine the synthesis of a mixed alkali metal derivative of $Na_2Mn_2S_3$: $Li_xNa_{2-x}Mn_2S_3$, and the results of high temperature reactions targeted to synthesize a similar phase. As a result, $LiNaMnS_2$ was identified and characterized by single crystal X-ray diffraction.

2. Experimental

Anhydrous acetonitrile, iodine, lithium foil (99.9%), sodium metal (99.8%) manganese powder (325 mesh 99.3%), and sulfur powder (325 mesh 99.5%) were purchased from Alfa Aesar and used as received. Liquid ammonia was distilled over sodium prior to use to remove residual water. Alkali metal sulfides (Li_2S_2, Na_2S_2) were synthesized by combining stoichiometric ratios of elements in liquid ammonia for reactive flux synthesis [15].

Disodium trithiodimanganate(II) ($Na_2Mn_2S_3$): 0.6559 g of Na_2S_2 (5.957 mmol), 0.6535 g of Mn (11.90 mmol), and 0.1910 g of S (5.957 mmol) were ground together under argon atmosphere in a glove box. This mixture was placed in alumina crucibles, sealed under vacuum in silica tubes, and ramped to 600 °C over a period of 12 h, held at temperature for another 12 h, and then cooled over 12 h. The air sensitive orange-red product was collected and stored under argon.

Sodium trithiodimanganate(II,III) ($Na_{2-x}Mn_2S_3$): 0.5971 g of $Na_2Mn_2S_3$ (2.369 mmol) was weighed into a Schlenck flask under argon with 20 mL of anhydrous acetonitrile. 0.3454 g of I_2 (1.361 mmol; slight excess) was added to the flask under positive argon pressure, and the mixture was heated with stirring to 60 °C for 15 min (until the solution returned to its original clear color). The powder was rinsed with anhydrous acetonitrile three times to remove byproduct salt and then dried under vacuum. The dark red-brown product was stored under argon for further use. Elemental analysis indicated that the product was incompletely oxidized yielding the formula $Na_{1.3}Mn_2S_3$.

Lithium sodium trithiodimanganate(II,III) ($Li_xNa_{2-x}Mn_2S_3$): 0.1310 g (0.5552 mmol) of $Na_{1.3}Mn_2S_3$ (the product of the previous reaction) was combined with 0.0047 g (0.6773 mmol) of Li in a Schlenck flask under an argon environment. Liquid ammonia (which was previously distilled over sodium) was cannulated into the flask, the reaction was stirred for 30 min, and the ammonia was allowed to evaporate while under positive argon pressure. The orange-red product was then collected and stored under argon. Elemental analysis revealed that the formula of the resulting product was $Li_{0.7}Na_{1.3}Mn_2S_3$.

The product of the above reaction, $Li_{0.7}Na_{1.3}Mn_2S_3$ was annealed by sealing the compound under vacuum in a silica tube and heating it to 600 °C following the heating procedure used to synthesize $Na_2Mn_2S_3$. The resulting orange-red mixture was characterized by powder X-ray diffraction and was found to contain $Na_2Mn_2S_3$, $LiNaMnS_2$, and MnS.

The synthesis of $LiNaMn_2S_3$ was also attempted using high temperature methods by grinding together 0.0825 g of Li_2S_2 (1.06 mmol), 0.1170 g of Na_2S_2 (1.063 mmol), 0.2340 g of Mn (4.260 mmol), and 0.0671 g of S (2.093 mmol). This mixture was then subjected to the same reaction conditions as $Na_2Mn_2S_3$. The orange-red product of this reaction was found to contain a mixture of $LiNaMnS_2$ and MnS.

Lithium sodium dithiomanganate(II) ($LiNaMnS_2$): 0.1308 g of Li_2S_2 (1.6777 mmol), 0.1841 g of Na_2S_2 (1.673 mmol), and 0.1843 g of Mn (3.355 mmol) were ground together in an argon environment. The mixture was then loaded into alumina crucibles, vacuum sealed in a silica tube, and subjected to the same reaction conditions as $Na_2Mn_2S_3$. The orange-red product of this reaction was found to be a mixture of $LiNaMnS_2$ and a trace amount of MnS.

Crystals of $LiNaMnS_2$ suitable for single crystal X-ray analysis were prepared by combining 0.1883 g of Li_2S_2 (2.414 mmol), 0.2665 g of Na_2S_2 (2.420 mmol), and 0.0664 g of Mn (1.209 mmol). This mixture contained a threefold molar excess flux of Li_2S_2 and Na_2S_2. This mixture was loaded into an alumina crucible, sealed in a silica tube under vacuum and heated to 600 °C over a period of 12 h, held at temperature for 48 h, and cooled to room temperature over a period of 60 h. The remaining flux was removed with dimethylformamide (DMF) yielding small hexagonally shaped air sensitive orange platelets.

3. Analysis

Powder X-ray diffraction data was collected using a Bruker D8 Focus diffractometer using a domed zero background air-tight holder over the range of 5–95° 2θ with a step size of 0.02° and an integration time of 13 s per step. Lattice parameters were computed through linear regression analysis from Le Bail fitting using the GSAS software package [16].

A single crystal diffraction intensity data set for $LiNaMnS_2$ was collected using a Nonius Kappa CCD instrument. Data was integrated using the Denzo software package [17], an analytical absorption correction was applied [18], and the structure was solved using direct methods with SHELXTL [19].

Samples for elemental analysis measurements by EDAX were prepared by sprinkling powdered sample onto carbon tape on a metal stub in an inert atmosphere glove box. These samples were transferred in sealed containers to the instrument, and quickly opened and transferred to the vacuum chamber of the SEM to minimize air exposure. EDAX measurements were taken using a JEOL 6400 FXV SEM equipped with an EDAX 6400F detector using high magnification (200,000 ×) for individual crystals as well as low magnification (50 ×) over many crystals to examine the possibility of inhomogeneous samples.

In order to prepare samples for ICP analysis, each sample was first washed three times with acetonitrile to remove any soluble residue from the crystals. ICP analysis was performed by digesting 10–40 mg of samples in concentrated aqua regia, and diluting solutions to a concentration range of 20–100 ppm in manganese. These solutions were analyzed in triplicate using a Spectro Ciros Vision spectrometer.

Molecular modeling calculations were completed using the Cerius 2 commercial software package. Default force field values were used, and the energy of the system was minimized in P1 symmetry.

4. Results and discussion

$Na_2Mn_2S_3$ was synthesized from a stoichiometric mixture of Na_2S_2, Mn, and S using the reactive flux method. Powder XRD analysis of $Na_2Mn_2S_3$ revealed no significant contaminant phases (Fig. 2a), and the refined unit cell constants (Table 1) closely match the previously published values $a = 14.942(2)$ Å, $b = 13.276(2)$ Å, $c = 6.851(2)$ Å, and $\beta = 116.50(1)^\circ$ [12]. The product was used without further treatment for subsequent reactions.

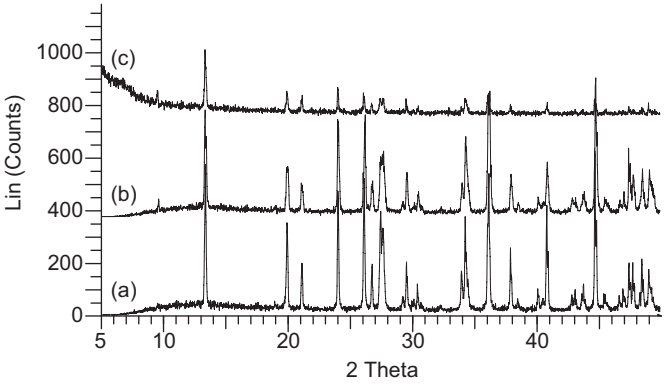

Fig. 2. Powder X-ray diffraction patterns of: (a) $Na_2Mn_2S_3$, (b) the oxidized product $Na_{2-x}Mn_2S_3$, and (c) the lithium intercalation product $Li_xNa_{2-x}Mn_2S_3$.

$Na_2Mn_2S_3$ was oxidized with iodine in acetonitrile in a manner similar to that used by Koizumi and coworkers [14]. Based on the general oxidation reaction:

$$Na_2Mn_2S_3 + x/2\ I_2 \rightarrow Na_{2-x}Mn_2S_3 + x\ NaI$$

Manganese may be oxidized from its initial oxidation state of +2 to the reported limiting value of +2.5 when $x = 1$ [14]. In practice, the brown color of the iodine solution was observed to fade to clear over a period of 5–10 min in a stirred, heated solution, and the thiomanganate color was observed to darken during this process. Subsequent powder XRD measurements of the oxidized product (following the removal of NaI by washing with acetonitrile) revealed a pattern very similar to that of $Na_2Mn_2S_3$ (Fig. 2b), and the refined unit cell constants of the product were comparable to the starting material (Table 1, listed as $Na_{2-x}Mn_2S_3$).

The surprising invariance of the $Na_2Mn_2S_3$ structure to oxidation is consistent with previous observations [14], yet further explanation is warranted as to why apparently half of the sodium ions may be deintercalated from the structure without causing a compression of the lattice. Simulation of this structure using the Cerius 2 software package revealed that the structure remained intact during energy minimization following the removal of all of the pseudo-tetrahedral sodium ions (site Na(1) Fig. 1), but the structure collapsed following the removal of the pseudo-octahedral sodium ions (sites Na(2) and Na(3) in Fig. 1). While this result must be considered qualitative at best since no attempts were made to optimize the force field values, it suggests that the tetrahedral Na(1) sites are not required to maintain the integrity of the structure, and instead these ions may be considered to be located in channel-like crevices within the thiomanganate layers. In this case, the deintercalation of these channel-like sodium ions would be expected to have little effect on the lattice parameters, consistent with results from deintercalation studies of other channel-type structures such as AV_6S_8 ($A = K$, Tl, In) [20–22]. We attempted to test this possibility by refining the sodium site occupancies from powder XRD data using the Rietveld method. This proved to be very challenging due to poor counting statistics (the compound began to decompose during measurements exceeding 12 h), and packing inhomogeneity which could not be avoided in the use of our air-free sample holder. Spherical harmonic refinement was used to address preferential orientation, and sodium site anisotropic displacement

Table 1
Summary of powder XRD data organized by structure-type.

	$Na_2Mn_2S_3$	$Na_{2-x}Mn_2S_3$	$Li_xNa_{2-x}Mn_2S_3$	Annealed $Li_xNa_{2-x}Mn_2S_3$
$Na_2Mn_2S_3$-type				
a-axis (Å)	14.9444(10)	14.9582(16)	14.9454(19)	14.9518(22)
b-axis (Å)	13.2770(8)	13.2860(12)	13.2815(12)	13.3075(13)
c-axis	6.8454(4)	6.8489(6)	6.8485(7)	6.8415(8)
α (deg)	90	90	90	90
β (deg)	116.527(4)	116.515(6)	116.531(6)	116.535(9)
γ (deg)	90	90	90	90
Volume (Å^3)	1215.25(15)	1217.94(22)	1216.27(24)	1217.86(25)
Refinement	$\chi^2 = 1.32$	$\chi^2 = 1.45$	$\chi^2 = 1.09$	$\chi^2 = 1.25$

	Annealed $Li_xNa_{2-x}Mn_2S_3$	Attempted direct synthesis: $LiNaMn_2S_3$	$LiNaMnS_2$
$LiNaMnS_2$-type			
a-axis (Å)	4.05376(23)	4.05496(19)	4.05119(24)
b-axis (Å)	4.05376(23)	4.05496(19)	4.05119(24)
c-axis	6.8063(4)	6.7930(4)	6.7791(5)
α (deg)	90	90	90
β (deg)	90	90	90
γ (deg)	120	120	120
Volume (Å^3)	96.863(14)	96.730(11)	96.353(15)
Refinement	$\chi^2 = 1.25$	$\chi^2 = 1.49$	$\chi^2 = 1.56$

parameters were constrained to be equal in order to reduce the number of independent variables. Unfortunately, sodium site occupancies (Na(1)–Na(3)) all refined to unrealistically high values in both $Na_2Mn_2S_3$ and the oxidized product $Na_{2-x}Mn_2S_3$. For example, when the Na(2) and Na(3) sites were set to full occupancy (1.00), the Na(1) site occupancy refined to the value 1.36 for $Na_2Mn_2S_3$, and to 1.46 for $Na_{1-x}Mn_2S_3$. It should be noted that the final refinement errors (w*R*p) were greater than 20% in each case, due primarily to the aforementioned problems with the samples. We are currently exploring other options for analysis (including the preparation of samples suitable for single crystal X-ray diffraction analysis) in order to resolve these problems.

ICP analysis of the product of the oxidation reaction yielded the formula $Na_{1.3}Mn_2S_3$ (based on the ratio of Na/Mn in the analyte). EDAX analysis revealed that there was a great deal of inhomogeneity within the sample. The ratio of Na/Mn in several small crystals was found to be close to 0.5 (indicating near-complete oxidation), while in some of the larger crystals the ratio was found to be as high as 0.8; the average formula by EDAX was found to be $Na_{1.37}Mn_2S_3$ for all of the measurements taken. Together these results indicate that oxidation was incomplete, which may be justified by considering that this reaction took place at 60 °C over a short time period. Ion migration through the lattice is expected to be slow under these conditions, and the oxidation of the exterior of each crystallite is expected.

The oxidized product $Na_{1.3}Mn_2S_3$ was reacted with elemental lithium dissolved in liquid ammonia in order to reductively intercalate lithium ions into the now-empty sodium sites. The general reaction (assuming complete reduction by lithium) is:

$$Na_{2-x}Mn_2S_3 + x\ Li \rightarrow Li_xNa_{2-x}Mn_2S_3$$

with $0<x<1$. During this reaction, the dark blue color of the lithium electride solution was observed to fade rapidly (within 5 min). Lithium was not observed to react with unoxidized $Na_2Mn_2S_3$ under identical conditions. Likewise, when excess lithium was added, this excess remained in solution following the reaction. The product of this reduction reaction was dried and analyzed by powder X-ray diffraction (Fig. 2c), yielding lattice constants that were again very similar to those of $Na_2Mn_2S_3$ (Table 2, listed as $Li_{0.7}Na_{1.3}Mn_2S_3$). This is not surprising, since the sites now occupied by lithium are presumably still large enough to accommodate an ion as large as sodium. Elemental analysis of this product was somewhat more difficult as lithium could not be detected by EDAX, but ICP analysis determined that the ratio of Li/Na was approximately 0.5 ($\pm$0.2), consistent with the anticipated formula $Li_{0.7}Na_{1.3}MnS_2$.

When the synthesis of $LiNaMn_2S_3$ (based on the ideal stoichiometry of the redox cycling reactions) was attempted using the reactive flux (high temperature) method, powder X-ray diffraction analysis revealed that a new product was obtained. Fig. 3 compares the X-ray diffraction data of the previously described lithium intercalated $Li_xNa_{2-x}Mn_2S_3$ (Fig. 3a) with other Li/Na/Mn/S preparations. MnS was identified as a byproduct at high temperatures (reflections are marked with asterisks in Fig. 3) along with another phase, which was indexed to a hexagonal unit cell with cell parameters (listed in Table 2) very similar to Li_2FeS_2 (with cell parameters $a = 3.902$ Å; $c = 6.294$ Å) [23] and the recently identified $NaLiZnS_2$ (with $a = 3.9711$ Å; $c = 6.7186$ Å) [24]. The formula $LiNaMnS_2$ is consistent with these results based on a possible decomposition reaction:

$$LiNaMn_2S_3 \rightarrow LiNaMnS_2 + MnS$$

Based on these findings, the synthesis of $LiNaMnS_2$ was attempted, and the resulting powder X-ray diffraction pattern (Fig. 3d) confirmed that this mixture produced the product with a reduced concentration of MnS. The synthesis was repeated using excess Li_2S_2 and Na_2S_2 flux to encourage the growth of crystals suitable for single crystal X-ray diffraction.

A single crystal of $LiNaMnS_2$ was selected, 1255 (108 independent) reflections were collected, and an analytical absorption correction was applied ($R_{int} = 0.0691$). Data were collected within a θ range of 3.01–27.16° to a completeness of 100.0% with a data index range of $-5 \leqslant h \leqslant 3$, $-4 \leqslant k \leqslant 5$, $-8 \leqslant l \leqslant 8$. A direct method solution in *P*-3*m*1 initially failed, but positions suitable for refinement were found by first generating a trial solution in space group *P*3. After shifting the origin and eliminating redundant positions, all atoms were refined aniosotripically in space group *P*-3*m*1 on F^2 for 11 variables with final electron density residuals of 0.242 and -0.528 eÅ^{-3} [19]. The results of the solution are displayed in Table 2 and Fig. 4. Further details of the crystal structure investigation are obtainable from Fachinformationszentrum Karlsruhe, Eggenstein-Leopoldshafen, Germany (Fax: +49 7247 080 666; *E-mail*: crysdata@fiz.karlsruhe.de) on quoting the depository number CSD-420221.

$LiNaMnS_2$ is isostructural to $LiNaCdS_2$ and $LiNaZnS_2$ [24]. The structure is composed of infinite planes of edge shared pseudo-tetrahedral metal sites which are occupied by a 50% mixture of lithium and manganese. These layers are separated by sodium cations in pseudo-octahedral coordination environments. Fig. 5 depicts the structure in a polyhedral form both parallel and perpendicular to the layering axis. The interatomic distances are comparable to those in closely related materials: Li/Mn–S

Table 2
Selected crystallographic data for $LiNaMnS_2$.

Space group	*P*-3*m*1
Formula weight	148.99
a (Å)	4.0479(6)
c (Å)	6.7759(14)
Z	1
V (Å^3)	96.15(3)
ρ, calc (g/cm^3)	2.573
Radiation wavelength (Å)	0.71073
Linear abs. coeff. (mm^{-1}) (calculated)	4.3700
Collection temp. (K)	153.2
*R*1[a] ($I>2\sigma$)	0.0175
w*R*2[b]($I>2\sigma$)	0.0367

[a] $R1 = \Sigma(|F_o|-|F_c|)/\Sigma|F_o|$.
[b] $wR2 = [\Sigma[w(F_o^2-F_c^2)^2]/\Sigma(w(F_o^2)^2)]^{1/2}$.

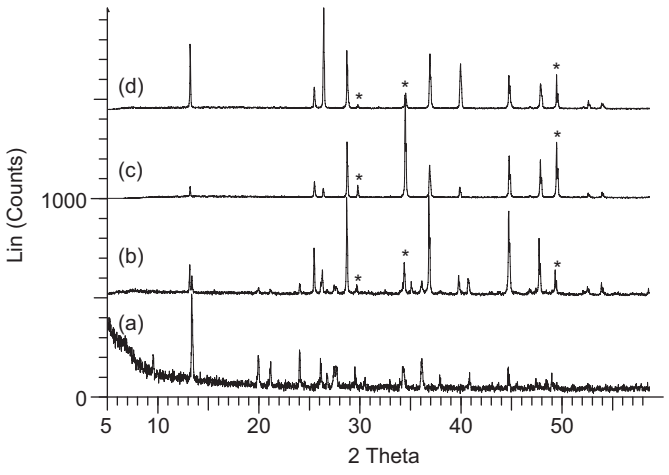

Fig. 3. Powder X-ray diffraction patterns of: (a) lithium intercalated $Li_xNa_{2-x}Mn_2S_3$, (b) lithium intercalated $Li_xNa_{2-x}Mn_2S_3$ after annealing to 600 °C, (c) attempted synthesis of $LiNaMn_2S_3$ from a reactive flux mixture, and (d) $LiNaMnS_2$. Diffraction pattern intensities were normalized for clarity, and major MnS reflections are marked with asterisks.

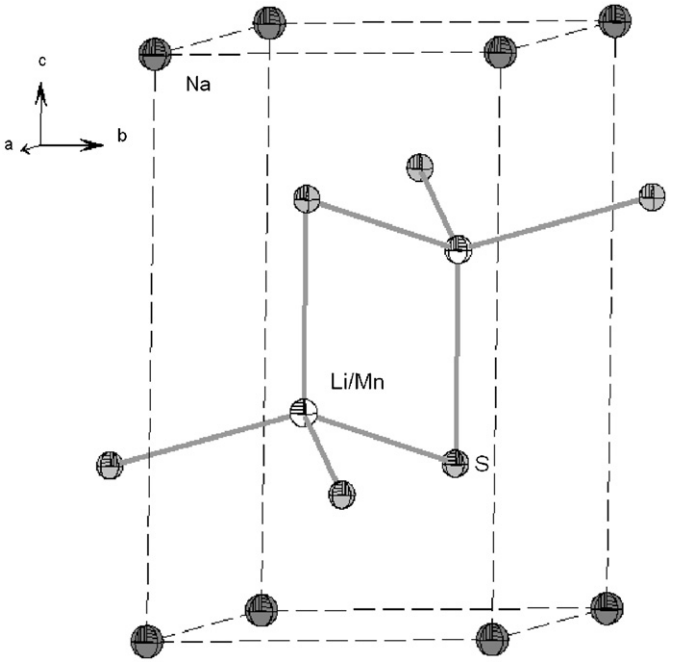

Fig. 4. Unit cell of $LiNaMnS_2$ drawn with 50% probability thermal ellipsoids. For clarity the complete coordination environments of the Li/Mn sites are included (only the two central sulfur sites are within the unit cell).

distances in $LiNaMnS_2$ range between 2.4427(4) and 2.4778(8) Å, which is very similar to the Li/Mn–S distance of 2.439(3) Å in $LiKMnS_2$ [25], and slightly longer than the Li/Zn–S distances of 2.5039–2.6051 Å in $LiNaZnS_2$ [24]. Na–S distances in $LiNaMnS_2$ are 2.9461(5), within the range of Na–S distances in $Na_2Mn_2S_3$ which are found between 2.68 and 2.96 Å [12], and nearly identical to the Na–S distances in $LiNaZnS_2$ of 2.9590 Å [23].

In order to complete the study of the lithium intercalated product $Li_{0.7}Na_{1.3}Mn_2S_3$, this compound was annealed to 600 °C and analyzed by powder X-ray diffraction (Fig. 3b). Three phases were identified: $Na_2Mn_2S_3$, MnS, and $LiNaMnS_2$. The refined lattice constants of the $LiNaMnS_2$ phase from this mixture are listed in Table 1. The proposed decomposition reaction is assumed to be responsible for the formation of MnS and $LiNaMnS_2$ from the lithium intercalated product, while residual $Na_2Mn_2S_3$ remained unaffected by annealing (control experiments confirmed that $Na_2Mn_2S_3$ was stable under the annealing conditions). Although it was not possible to confirm the composition of the mixture by quantitative X-ray analysis due to the poor crystallinity of the sample, the decomposition of $Li_{0.7}Na_{1.3}Mn_2S_3$ is expected to produce $Na_2Mn_2S_3$, MnS, and $LiNaMnS_2$ in an approximate 1:2:2 molar ratio, respectively, based on stoichiometric balance.

5. Conclusions

For structures containing oxidizable species like Mn^{+2}, I_2 is a convenient reactant for the oxidative deintercalation of alkali metal ions from a structure. The resulting alkali metal iodide salt may be easily removed (as opposed to the byproducts of oxidizing agents like $KMnO_4$), and the product may be used for further reaction. In the present work, when $Na_2Mn_2S_3$ was treated with I_2, the unit cell of the oxidized product $Na_{2-x}Mn_2S_3$ surprisingly was not affected by the reaction. Additionally, based on elemental analysis the oxidation reaction was determined to be incomplete, resulting in an average formula of $Na_{1.3}Mn_2S_3$ rather than the ideal formula $NaMn_2S_3$. Since powder X-ray diffraction was of limited use in the analysis of the oxidized product, the best

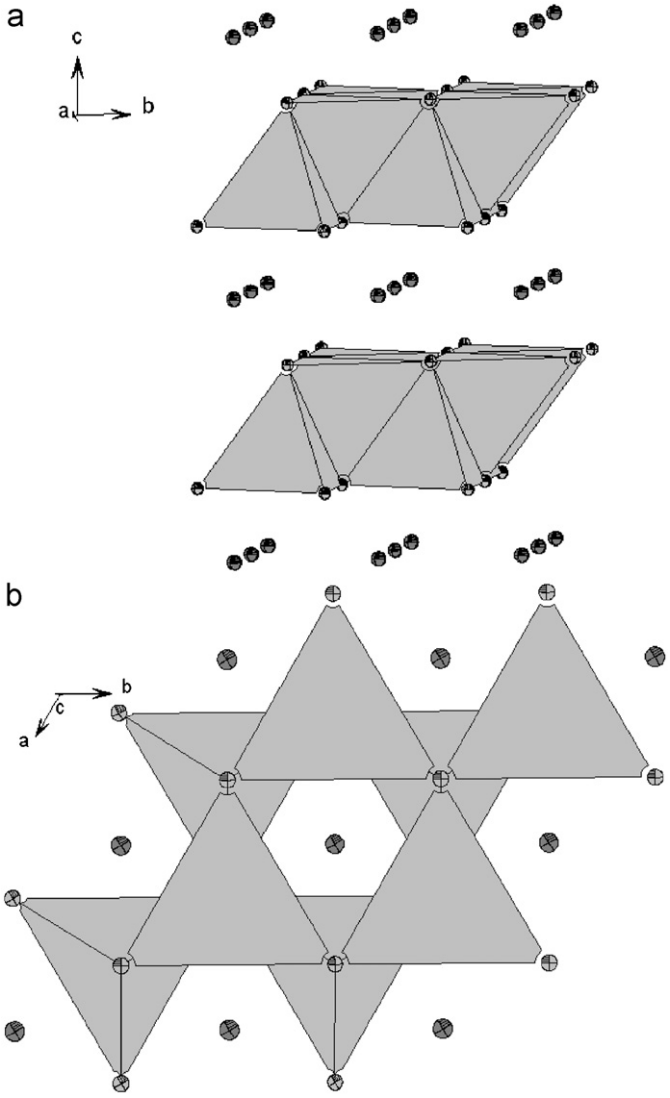

Fig. 5. Polyhedral representations of $LiNaMnS_2$: (a) viewed along the *a*-axis, parallel to the Li/MnS_2^{-1} layers and (b) viewed along the *c*-axis, perpendicular to the Li/MnS_2^{-1} layers.

solution to this problem is to synthesize crystals of $Na_2Mn_2S_3$ suitable for single crystal analysis, and to perform oxidation reactions upon these samples to assess the effects on site occupancies. However, this may change the results of the redox cycling process due to the change in kinetics caused by the decrease in crystal surface area. Solid state electrochemical studies on this system may be used to develop a model of the reaction kinetics for a given sample. These measurements would also provide insight into the ionic conductivity of the oxidized product, which is anticipated to be relatively high due to the large number of ion vacancies.

The reductive intercalation of lithium cations into $Na_{1.3}Mn_2S_3$ yielded a product with the formula $Li_{0.7}Na_{1.3}Mn_2S_3$, with lattice parameters nearly identical to those of $Na_2Mn_2S_3$. When the reduced product was annealed, partial decomposition occurred to yield MnS, residual $Na_2Mn_2S_3$, and a new structure, $LiNaMnS_2$. $LiNaMnS_2$ is isostructural to $LiNaCdS_2$, but it may also be related to $LiKMnS_2$ [25], composed from an edge-shared tetrahedral Li/MnS_2 layered framework separated by potassium ions which occupy cubic sites between the layers (as opposed to the octahedral sodium sites in $LiNaMnS_2$), as well as $LiCuFeS_2$, in which the mixed metal tetrahedral sites are occupied by Cu/Fe

rather than Li/Mn [26]. The observation of $LiNaMnS_2$ further ties together the structural relationship of the metals Mn, Fe, Co, and Zn in mixed metal sulfides, which are all known to form isostructural compounds $NaCuMS_2$ [27]. By analogy, it is extremely likely that undiscovered compounds such as $LiNaFeS_2$ and $LiCuMnS_2$ should also crystallize in this structure-type. This extended class of compounds may be of interest for further study for intercalation and ion mobility studies.

Acknowledgments

We thank Gary Steinmetz at the Texas Parks and Wildlife Environmental Contaminants Laboratory for his help with ICP analysis, and Anup Bandyopadhyay for his help with EDAX measurements. Financial support from the Petroleum Research Fund (Grant 41834-GB10) and the National Science Foundation (Grant IO 8-804) are gratefully acknowledged.

References

[1] A. Patil, V. Patil, D. Wook Shin, J.-W. Choi, D.-S. Paik, S.-J. Yoon, Mater. Res. Bull. 43 (2008) 1913–1942.
[2] J. Molenda, J. Mater. Sci. 24 (2006) 61–67.
[3] J. Thomas, Nat. Mater. 2 (2003) 705–706.
[4] O.J. Rutt, T.L. Hill, Z.A. Gal, M.A. Hayward, S.J. Clarke, Inorg. Chem. 42 (2003) 7906–7911.
[5] A. Lappas, C.J. Nuttall, Z.G. Fthenakis, V.Y. Pomjakushin, M.A. Roberts, Chem. Mater. 19 (2007) 69–78.
[6] P. Joensen, R.F. Frindt, S.R. Morrison, Mater. Res. Bull. 21 (1986) 457.
[7] C. Barriga, P. Lavela, J. Morales, J. Pattanayak, J.L. Tirado, Chem. Mater. 4 (1992) 1021–1026.
[8] R. Moshtev, V. Manev, A. Nassalevska, A. Gushev, J. Power Sources 26 (1989) 285–292.
[9] M. Holzapfel, M. Strobele, H.-J. Meyer, Z. Anorg. Allg. Chem. 627 (2001) 2654–2656.
[10] L. Iordanidis, M.G. Kanatzidis, Angew. Chem. 39 (2000) 1928–1930.
[11] J.K. Guy, R.E. Spann, R.R. Martin, Solid State Ionics 179 (2008) 409–414.
[12] K. Klepp, P. Böettcher, W. Bronger, J. Solid State Chem. 47 (1983) 301–306.
[13] J. Kim, T. Hughbanks, J. Solid State Chem. 146 (1999) 217–225.
[14] S. Kikkawa, H. Taira, M. Koizumi, Synth. Met. 19 (1987) 897–900.
[15] M.G. Kanatzidis, Chem. Mater. 2 (1990) 353–363.
[16] A.C. Larson, R.B. Von Dreele, Los Alamos National Laboratory Report no. LAUR 86-748, 2000.
[17] Z. Otwinowski, W. Minor, in: C.W. Carter, R.M. Sweet (Eds.), Methods in Enzymology, Academic Press, New York, 1997, pp. 307–326.
[18] N.W. Alcock, Acta Cryst. A. 26 (1970) 437–439.
[19] SHELXTL 5.1; Bruker AXS Inc., Madison, WI, 1998.
[20] W. Bensch, J. Koy, M.J. Wesemann, Alloys Compd. 178 (1992) 193–204.
[21] K.D. Bronsema, G.A. Wiegers, Mater. Res. Bull. 22 (1987) 1073–1080.
[22] A.B. Garg, V. Vijayakumar, B.K. Godwal, T. Ohtani, B.R. Martin, H.D. Hochheimer, Solid State Commun. 132 (2004) 731–736.
[23] R.J. Batchelor, F.W.B. Einstein, C.H.W. Jones, R. Fong, J.R. Dahn, Phys. Rev. B 37 (1998) 3699–3702.
[24] B. Deng, G.H. Chan, F.Q. Huang, D.L. Gray, D.E. Ellis, R.P. Van Duyane, J.A. Ibers, J. Solid State Chem. 180 (2007) 759–764.
[25] D. Schmitz, W. Bronger, Z. Krist. 174 (1986) 177–179.
[26] R. Fong, J.R. Dahn, R.J. Batchelor, F.W.B. Einstein, C.H.W. Jones, Phys. Rev. B 39 (1989) 4424–4429.
[27] M. Oledzka, K.V. Ramanujachary, M. Greenblatt, Chem. Mater. 10 (1998) 322–328.